International Journal of Greenhouse Gas Control 102 (2020) 103162

Contents lists available at ScienceDirect

International Journal of Greenhouse Gas Control

journal homepage: www.elsevier.com/locate/ijggc

Characterization of CO_2 self-release during Heletz Residual Trapping Experiment I (RTE I) using a coupled wellbore-reservoir simulator

Farzad Basirat [a,*], Zhibing Yang [b], Jacob Bensabat [c], Stanislav Levchenko [c], Lehua Pan [d], Auli Niemi [a]

[a] Department of Earth Sciences, Uppsala University, Villavägen 16, SE-75236, Uppsala, Sweden
[b] State Key Laboratory of Water Resources and Hydropower Engineering Science, Wuhan University, Wuhan, 430072, China
[c] Environmental and Water Resources Engineering –EWRE Ltd., Haifa, Israel
[d] Energy Geosciences Division, Lawrence Berkeley National Laboratory (LBNL), Berkeley, CA, USA

ARTICLE INFO

Keywords:
CO_2 injection experiment
Residual trapping
Coupled wellbore-reservoir
CO_2 self-release
Numerical modeling

ABSTRACT

In order to quantify CO_2 residual trapping *in situ*, two dedicated single-well push-pull experiments have been carried out at the Heletz, Israel pilot CO_2 injection site. Field data from some parts of these experiments suggests the important effect of the hydrodynamic behavior in the injection-withdrawal well. In the present work a model capturing the CO_2 transport and trapping behavior during Heletz Residual Trapping Experiment I is developed, with a special focus on coupled wellbore-reservoir flow. The simulation is carried out with the numerical simulator T2Well/ECO2N (Pan et al. 2011) which considers the wellbore-reservoir coupling. Of particular interest is to accurately model the period when the well is open to the atmosphere and self-producing CO_2 and water in a geyser-like manner. It is also of interest to identify what conditions are causing the oscillating pressure-temperature behavior and the associated periodic gas-liquid releases, as well as to determine the amount of gas lost from the reservoir during this period. The results suggest that the behavior is due to cyclical CO_2 exsolution from the aqueous phase along with a reduction of mobility of both CO_2 and brine in the near wellbore-reservoir area, the latter being due to a zone of dispersed CO_2 bubbles near the wellbore. This behavior could be successfully captured with a new set of relative permeability functions developed earlier for CO_2 exsolution in laboratory experiments (Zuo et al., 2013).

1. Introduction

Residual or capillary trapping is an important trapping mechanism in geological storage of CO_2 (Niemi et al., 2017; Rasmusson et al., 2014). It is defined as immobilization of individual bubbles or relatively small blobs of the CO_2-rich phase by capillary forces in local trapping structures, or being stuck in dead-end pore spaces (Zhang et al., 2011). Being able to characterize and quantify the residual trapping at a given site is important as it is crucial to the eventual total capacity of a reservoir to trap CO_2.

One of the main parameters that describes residual trapping is residual gas saturation (S_{gr}). In spite of the importance of this parameter, very few studies so far have attempted to determine it *in situ*. Recent reviews summarizing works to determine this parameter *in situ* are given in Krevor et al. (2015) and in Niemi et al. (2017) and below only those studies relevant to the present work are referenced. Zhang et al. (2011) designed a single-well push-pull experiment sequence to quantify the maximum residual gas saturation of supercritical CO_2 ($ScCO_2$) in a saline aquifer. This experiment was carried out at Otway, Australia, in 2011 (Paterson et al., 2013) and the interpretation is presented in Haese et al. (2013) and LaForce et al. (2014). An additional experiment following a similar principle was carried out at Otway in 2015–2016 (Ennis-King et al., 2017). Developing further the concepts developed for Otway, (Rasmusson et al., 2014) in turn presented three alternative push-pull test-designs as preparation to the experiments to be conducted at the Heletz site, Israel (Niemi et al., 2012; Niemi et al., 2016). These experiments, carried out in 2016 and 2017, are presented in detail in Niemi et al., 2020, this issue) and the interpretation of the residual saturations based on the two experiments by means of reservoir modeling in Joodaki et al. (2020a, b).

The principle of Heletz CO_2 residual trapping experiments was to create a residually trapped zone of CO_2 *in situ*, and to use different

* Corresponding author at: Department of Earth Sciences, Uppsala University, Villavägen 16, SE-75236, Uppsala, Sweden.
E-mail address: farzad.basirat@geo.uu.se (F. Basirat).

https://doi.org/10.1016/j.ijggc.2020.103162
Received 4 June 2019; Received in revised form 29 April 2020; Accepted 7 September 2020
Available online 21 September 2020

characterization tests (hydraulic, tracer and thermal tests) before and after creating this zone. The difference in the outcome of these characterization tests provides information of the residually trapped zone (Niemi et al., 2016; Rasmusson et al., 2014). In the first experiment, the Residual Trapping Experiment I (RTE I), carried out in September 2016, the residually trapped zone was created by first injecting CO_2, then withdrawing the mobile CO_2 leaving the residually trapped CO_2 behind. The CO_2 withdrawal stage consisted of two parts, a self-release part and a period of active pumping. During the self-release stage, the well was opened to the atmosphere and CO_2 was spontaneously releasing in a geyser-like pattern, first only CO_2, then CO_2 with water. During the self-release stage, the pressure and temperature measurements at the reservoir depth show cycling fluctuation. As it is important to fully understand the amount of CO_2 lost from the reservoir during the self-release period, a detailed well-reservoir model was built to present the system, to study this period. During the following active pumping stage, fluids were pumped out with airlift technique until the formation was deemed to be at residual stage.

The observed cyclic variation in pressure and temperature is very similar to the eruptive behavior observed in a CO_2-driven geysering well (Lu et al., 2005, 2006; Watson et al., 2014). The term geyser is used to describe the natural phenomena observed in geothermally active areas where hot water and steam are periodically ejected into the atmosphere (Lu et al., 2005). However, in some deep wells that erupt like geysers, eruption of water and CO_2 at temperatures below 100 °C have also been observed to discharge periodically. This type of geysering is known as CO_2-driven cold-water geysers, such as geothermal wells at Te Aroha in New Zealand (Lu et al., 2006; Michels et al., 1993), Crystal and Tenmile geysers in Utah (Gouveia and Friedmann, 2006; Han et al., 2013; Ross, 1997), and Chimayo geyser in New Mexico (Lu et al., 2006; Watson et al., 2014). In natural CO_2-driven geysers, the eruption of water is the result of degassing (exsolution) of CO_2-rich fluids through wellbore due to hydrostatic pressure reduction (Lu et al. 2005). The mechanism of CO_2-driven geyser is described in detail by Lu et al. (2006), and can be summarized as follows. A cycle starts when the water level in a well leading up to the surface has recovered from an earlier low level and reaches the top of the well. The pressure in the well then has its maximum value and temperature its lowest. CO_2 gas bubbles are formed due to exsolution of CO_2 from oversaturated water in the wellbore. The depth where CO_2 in aqueous phase starts to exsolve is called the flash depth (FD), and is defined by the prevailing pressure and temperature at that point. The exsolved CO_2 bubbles migrate upwards due to the lower density of CO_2 gas in comparison to that of liquid water. During the upward migration of the CO_2 gas, the small bubbles start merging and create larger bubbles and slug flow. The formation of slug flow in turn causes water flow out of the wellbore. The water eruption continues and reduces the hydrostatic pressure, and consequently the FD in the well deepens. Finally, the CO_2 exsolution depth will reach its maximum depth, *i.e.* the well chamber. Due to degassing, eruptions will cease once the CO_2 concentration in the aqueous phase has reached a critical minimum, and needs to wait for completion of CO_2 by another recharge from the reservoir. This process of CO_2-driven eruption shows both self-enhancing and self-limiting behavior, resulting in the periodic eruption observed in geothermal reservoirs (Watson et al., 2014).

The model simulations by Lu et al. (2006) could reproduce all the important characteristics of geysering flow, such as periodic fluid discharge from the wellhead and the periodic variation in fluid pressure and gas saturation at different depths in the well. Similarly, Pruess (2008) carried out simulations for leakage scenarios for a potential of self-enhancement of CO_2 discharges from a CO_2 reservoir. The results showed both self-enhancing and self-limiting features. Pan et al. (2011a) in turn studied an eruptive CO_2 leakage behavior from a reservoir near residual saturation by means of a coupled reservoir-wellbore model.

In this paper, the focus is on modeling the CO_2/water self-release process observed during Heletz Residual Trapping Experiment, similar to the behavior discussed above. This self-release of CO_2 as such causes uncertainty in the CO_2 mass balance when the processes in the reservoir are modelled and needs to be addressed in detail to get a proper estimate of CO_2 lost into the atmosphere. In addition, understanding and rigorously modeling this complex process also furthers the overall understanding of processes in the reservoir and wellbore during a CO_2 injection-withdrawal experiment. For the modeling, we use the coupled wellbore-reservoir simulator T2Well-ECO2N (Pan and Oldenburg, 2014; Pan et al., 2011b) that has been specifically developed for geological storage of CO_2. In the following text, we will first shortly describe the relevant parts of the Heletz RTE I carried out in 2016. We then proceed to the data analysis, model development and numerical simulations with well-reservoir simulator T2Well-ECO2N. This is followed by an analysis of the results, discussion and conclusions.

2. Methodology and analyses

2.1. Field data

The Heletz pilot CO_2 injection site is part of a depleted oil field located in the southern Mediterranean coastal plain of Israel. The target formation, perforated for CO_2 injection, consists of two sandstone layers, separated by low-permeability shale. At the injection well, H18A, which was used for the residual trapping experiments, the top of the formation is at the depth of 1627 m. The thicknesses of the sandstone layers are 2 and 9 m and the thickness of the separating shale layer is 3 m. The well is instrumented for CO_2 and water injection and fluid withdrawal, as well as instrumented with downhole pressure and temperature sensor (located at depths 1617.35 m and 1632.9 m), with optical fiber for temperature measurement as well as U-tube for fluid sampling. A full description of the site and the instrumentation can be found in Niemi et al. (2016).

The first Heletz residual trapping experiment (RTE I) which is the focus in the present work, took place between 9th and 29th of September 2016. The measured pressure sequence in the two down-hole pressure sensors are shown in Fig. 1. The Figure shows the time period of creating the residually trapped zone of CO_2, from the start of the CO_2 injection to the end of the pumping-out period. The reference hydraulic tests before and after creating the residual zone are not shown here but are discussed, as is the entire test, in Niemi et al., 2020 this issue) and Joodaki et al. (2020a, b).

In this work the focus is in the CO_2 self-release period. After CO_2 injection and some following rest period, the well was opened to the atmosphere to initiate the fluid withdrawal. Between 21st and 24th of September the well was open to the atmospheric pressure allowing fluids, both CO_2 and water, to be released to the surface. This self-release of water and gas continued in periodic pulse releases of fluids which was associated with abrupt fluctuation of pressure and temperature during this period (Fig. 2). At the very early stage (before 21th of September 15:00) only CO_2 was released, followed by a period of geyser-like eruptions of both water and CO_2.

At the top of the well, the released fluids were led to a water tank where CO_2 was released to the atmosphere while water flow rate was measured with a flow meter. The water flow rate was corrected for the effect of the storage tank by continuously following the water level in the tank by means of a pressure sensor at the bottom of the tank (for details see Niemi et al., 2020, this issue). The CO_2 flow rate could not be measured with the setting available.

The modeling work here is especially focused on the period where somewhat unexpectedly both CO_2 and water are being released in a geyser-like cyclic pattern (22nd to 24th of September). The short period before that (Sept 21st) where only CO_2 was released represents a different type of process and is mainly CO_2 coming from the well.

2.2. Modeling approach

Two approaches have been used for analyzing the behavior during

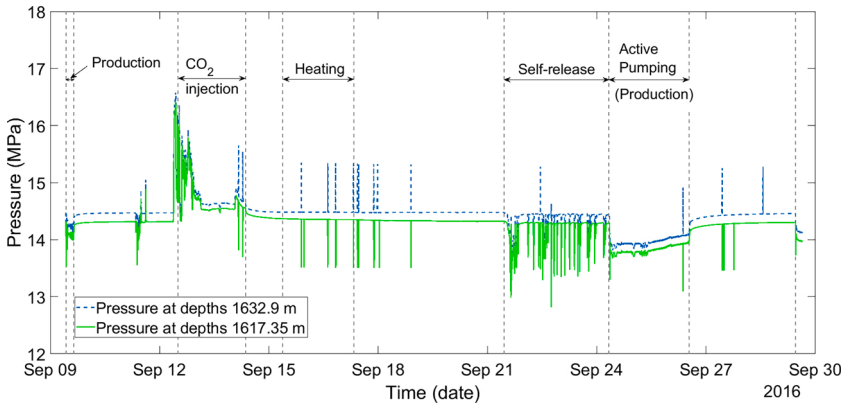

Fig. 1. Measured pressure at downhole sensors during time period September 9th to September 30th, Heletz Residual Trapping Experiment I.

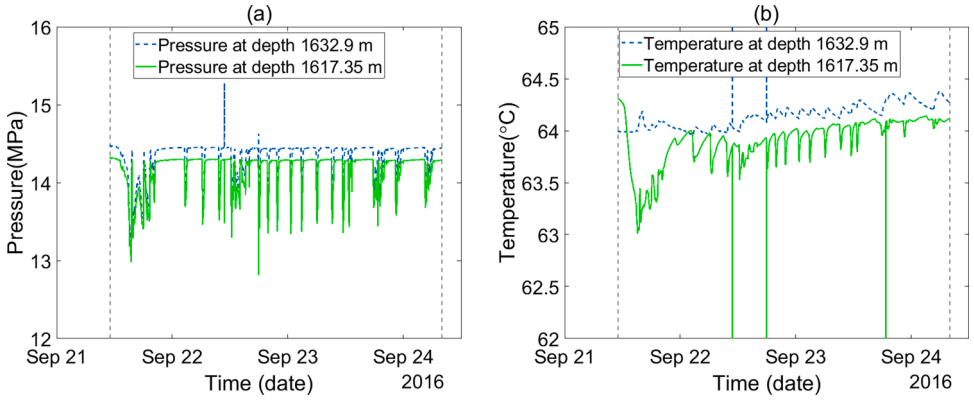

Fig. 2. (a) Measured pressure and (b) measured temperature during the self-release period. Solid lines show measurements at 1617.35 m depth and dashed lines show measurements at 1632.91 m depth sensors.

the self-release stage. First, the coupled reservoir-well simulator T2Well/ECO2N was used to understand the influence of reservoir properties on pressure response. Second, a 1D numerical model of the well alone was used to estimate the amount of CO_2 and water discharged through the self-release process. Both simulations were carried out with T2Well/ECO2N simulator (Pan et al., 2011b).

2.2.1. Analysis of CO_2 volume fraction

Pressure and temperature were monitored at two depths at the well bottom, at the depth of the target reservoirs. Sensor PT-76 was located at the depth of 1632.91 m and sensor PT-78 at the depth of 1617.35 m, inside the well chamber and outside the well tubing. It has to be mentioned that Sensor PT-78 was located above the well screen (Fig. 3a). The pressure difference between the two sensors can be used to determine the mixture (CO_2 and water) density and thereby the volume fractions of CO_2 and water in the well chamber between the two sensors. This can be done by using a simple approach suggested by Lu et al. (2005), where the pressure difference between two points allow us to determine the mean density of the fluid mixture and its local average gas saturation by means of the following equations:

$$\rho_m = \frac{P_{76} - P_{78}}{gh} \tag{1}$$

$$\alpha = \frac{(\rho_L - \rho_m)}{(\rho_L - \rho_G)} \tag{2}$$

where α is the gas saturation fraction, ρ_L is the brine density, ρ_G is the CO_2 density, g is the gravitational acceleration, and h is the distance between the two pressure sensors. The density of brine (ρ_L) in current reservoir conditions (brine salinity of 52,502 mg/l and temperature about 64 °C), is 1019.2 kg/m^3. In the present calculations, the value for the liquid density ($\rho_L =$ 1022.2 kg/m^3) and the value for the CO_2 density ($\rho_G =$ 533.0 kg/m^3) are used, which corresponds to average prevailing pressure, temperature and salinity conditions of 14.5 MPa, 64 °C, and 52.5 *g*/l at Heletz, reservoir depth.

2.2.2. Numerical simulator T2Well/ECO2N

T2Well is an extended version of TOUGH2 numerical simulator for modeling non-isothermal, multi-phase, multicomponent fluid and energy flow in a coupled well-reservoir system (Pan and Oldenburg, 2014; Pan et al., 2011b,c). The multiphase flow in the wellbore is simulated by solving the one-dimensional momentum equation. The velocity of the two-phases is described by DFM (Drift Flux Model) (Shi et al., 2005). By applying the DFM, the two-phase momentum equations are lumped into a single momentum equation for fluid mixture. A summary of the mathematical formulations that are implemented in T2Well can be found in the T2Well/ECO2N manual (Pan and Oldenburg, 2014). Like TOUGH2, T2Well needs to be used with different equations-of-state (EOS) modules to describe different fluid mixtures. In this work, we use the module ECO2N that includes equations-of-state for two-phase flow (gas and liquid), three mass components (water, salt, and CO_2) over the ranges of pressure and temperature of interest in this study. In ECO2N, the term 'gas phase' refers to the CO_2-rich phase and the term 'liquid phase' refers to the water-rich phase. It should be noted that CO_2 in 'gas phase' could formally be gaseous, liquid, or, supercritical CO_2, depending on the pressure and temperature conditions. However, by our terminology CO_2 in the liquid phase is CO_2 dissolved in water or brine. It should further be pointed out that the model is based on the assumptions of equilibrium dissolution of CO_2 in brine, and of constant residual gas saturation parameter (S_{gr}). The application of T2Well for CO_2 as the gas

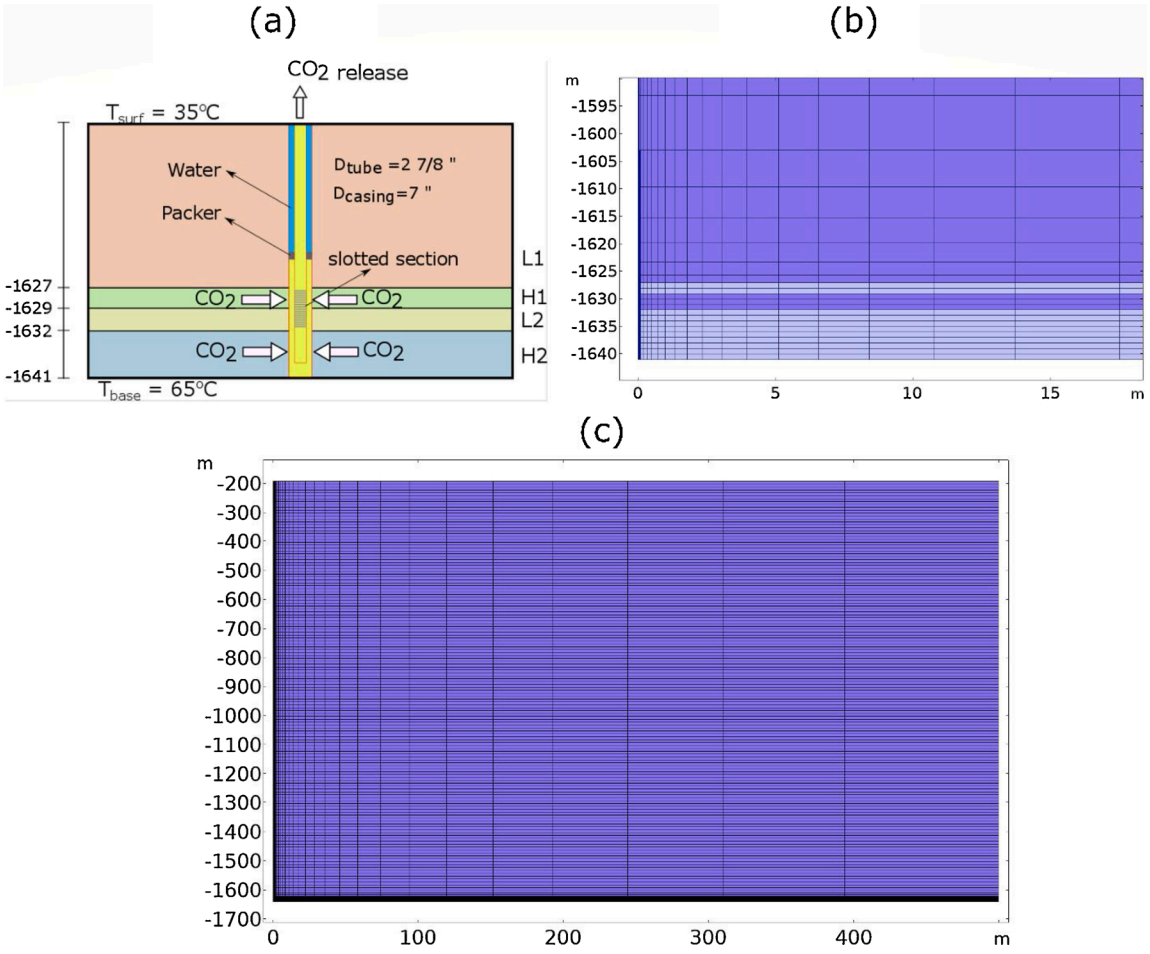

Fig. 3. (a) Conceptual model (not to scale) showing Heletz test reservoirs (H1 and H2), low permeable layers (L1 and L2), and wellbore for CO_2 self-release period, (b) the mesh resolution near the well and reservoir layers, and (c) the Radially symmetric grid for modeling coupled well-reservoir system in Heletz.

phase and water flow in a vertical pipe has been verified and validated with analytical solution and the field data by Pan and Oldenburg (2014) and Pan et al. (2018).

2.2.2.1. Conceptual model and model development. The conceptual model (Fig. 3) representing the site was constructed based on the available geological and petrophysical data. The model and the parameter values are based on the site characterization data available (Niemi et al., 2016) as well as results and calibration from the previous reservoir model analyzing the Residual Trapping Experiment I (Joodaki et al., 2020a). The parameter values are summarized in Table 1. The model consists of two high-permeability layers (noted here as H1 and H2), 2 and 9 m thick, respectively, separated by a 3 m thick low-permeable layer (L1), overlain by an additional low-permeable layer (L2). The bottom depth is at 1641 m, and the top of model is at 194 m below ground level, which corresponds to the level of the groundwater table. The top of model is considered at 194 m below ground level to avoid the complexities of the unsaturated zone and the presence of the air component in the numerical modeling. The layers above the actual reservoir layers were considered only in terms of how they influence the heat transfer from and into the well. At the top boundary, at 194 m below the ground level, a specified pressure boundary condition equal to atmospheric pressure is specified. At this boundary we also assume a constant temperature of 35 °C. The reason why we could not model the part above the water table is that the well model we use (T2Well) can account for CO_2 and water but not air as the third fluid. An impermeable layer with a constant temperature of 65 °C is assigned to the bottom boundary. The thermal properties of surrounding rocks are assumed homogeneous for all rock types.

Table 1
Properties and parameter values used for the modeling.

Parameter	Value	Unit
Well Length	1448	m
Well Diameter	0.073	m
Thermal conductivity	3.30	W/m C°
Reservoir radius	1000	m
Boundary conditions at wellhead	P = 0.1035 T = 35	MPa C°
Roughness parameter	0.046×10^{-3}	M
Absolute permeability	H1 = 650 H2 = 450	mD mD
Porosity	H1 = H2 = 0.25	
Salinity	0.05	NaCl mass fraction
Initial conditions	Gas saturation, pressure and temperature at the end of rest time (at 21-sep-2016 11:15) from numerical simulation.	
Outer boundary condition	No-flow	

A radially symmetric grid was used with a grid spacing of 0.0365 m representing the wellbore, and with 45 logarithmically increasing grid blocks out to 500 m in radial direction. In vertical direction 10 m grid blocks were used down to the depth of 1604 m and 1 m grid blocks were used for the reservoirs and the low permeable shale layer in between

(L2). It should be pointed out that the numerical stability of the simulations depends on the number of the grid blocks used. When using a very fine mesh, convergence problems occurred. The current mesh (Fig. 3a) is the finest we could use and achieve numerical convergence. The current mesh has considerable refinement near the area that reservoir and wellbore are connected and we believe the mesh to be sufficiently fine so that a further refinement of the mesh would not change the overall results.

To obtain the initial and boundary conditions, a numerical simulation for the sequences of CO_2 injection, and the following rest period (from 12th of September 12:00 to 21st of September 11:05) were carried out first with the same mesh and parameter values as given in Table 1. It should be noted that there is a heating period from 15th of September 8:45 to 17th of September 8:20. This is part of the overall test sequence and important in determining the residual saturation. For the present analysis, however, the temperature effects are not significant.

Fig. 4 shows the simulated pressure along with the measured data for the period before opening the well. It can be seen that the model does not capture the variations during water and tracer injection, which are believed to be due to borehole skin effects and accumulation of sand in the wellbore during these early stages of the injection. These are not the focus in the present study and will be not further analyzed here (see Joodaki et al., 2020a). The behavior during the CO_2 injection and pressure evolution after that are deemed to be sufficiently captured by the model so that the result can be used as initial condition in reservoir for simulating the period when well is open to the atmosphere.

2.2.2.2. CO_2 mobility models. Relative permeability functions are critical for all two-phase flow systems and especially crucial when estimates on residual trapping are made. In the Heletz case, core measurements on relative permeability have been made (Hingerl et al., 2016) and the obtained curve is presented in Fig. 5 (dashed lines).

As already discussed above, the pressure measurements (Fig. 2) during the self-release period indicated a geyser-like behavior. Based on field observations of natural geysers, the CO_2 in the reservoir is in dissolved form and the released, mobile CO_2 observed at the top of the well is the result of CO_2 exsolution from the saturated water, due to the lowering of the pressure as discussed above. The numerical simulations by Pan et al. (2011a) concerning transient CO_2 leakage through a well on the other hand showed that the gas saturation in the reservoir is only slightly above the residual gas saturation for the geysering behavior to happen. In our case, the CO_2 inside the reservoir is not yet at residual (immobile) state during the self-release period, at least not for the entire region, as the observations during the active pumping stage (the next sequence in RTE I) again show presence of mobile CO_2. The mobility of CO_2 appears, however, to be reduced during the period of self-release and associated exsolution. Interestingly, Zuo et al. (2013) carried out

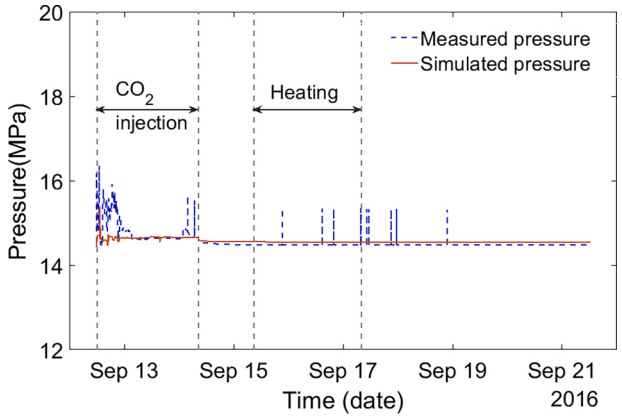

Fig. 4. Measured pressure and numerically modelled pressure (at depth of 1632.91 m) along with test sequences.

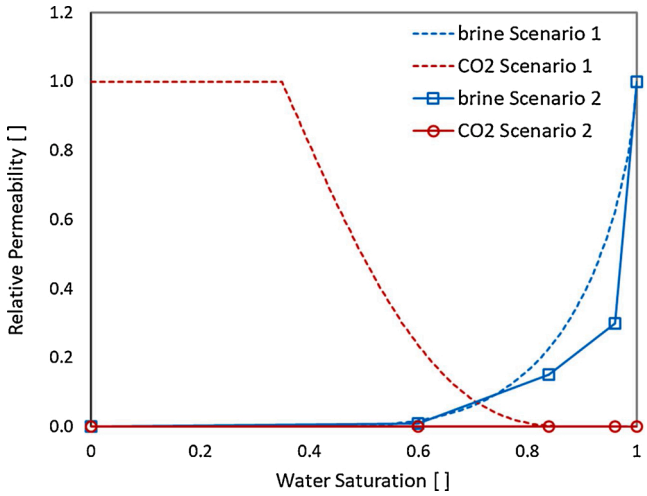

Fig. 5. Relative permeability of CO_2 and brine used in numerical simulation of CO_2 self-release. The lines without markers are based on core data from Heletz [scenario 1] (Hingerl et al., 2016; Niemi et al., 2016) and the lines with markers show the reduced relative permeabilities based on Zuo et al. (2012) [scenario 2].

laboratory experiments concerning the effect of exsolution of CO_2 on the relative permeability of the gas and the liquid. Their finding was that both mobilities were significantly reduced. The corresponding relative permeability functions are presented in Fig. 5 with solid lines. It should be noted that while even the relative permeability of brine is strongly reduced in comparison to the base case (dashed lines in Fig. 5), the relative permeability of CO_2 is reduced to zero. The physical reason for gas mobility becoming zero is according to Zuo et al. (2012) the pressure (and temperature) reduction induced exsolution and the exsolved CO_2 creating disconnected CO_2 bubbles. These bubbles, while causing higher gas saturation are disconnected from each other and therefore immobile. Furthermore, these bubbles block the flow of water and thereby reduce the water permeability as well.

In our simulations, we use both the original relative permeability functions determined on the cores and the exsolution-reduced relative permeabilities presented by Zuo et al. (2012, 2013). The relative permeability presented by Zuo et al. (2013) then describes a situation where only dissolved (no free) CO_2 can enter to the well-bottom.

3. Results

3.1. Analysis of CO_2 volume fraction

Fig. 6 shows the measured pressure difference and the estimated volume fraction of CO_2 (or gas saturation) between the two sensors in the wellbore during the self-release stage. The pressure difference fluctuates considerably. According to Eq.s (1) and (2), a smaller pressure difference corresponds to a larger CO_2 volume between the two sensors and *vice versa*. The gas saturation in the wellbore ranges between 0.04 and 0.31. There are two possible sources for the gas in the wellbore: CO_2 exsolution from oversaturated carbonated water and gaseous CO_2 in the reservoirs. The contributions of the two sources to the CO_2 gas volume in the column between two sensors cannot be determined. Because of the completion of the well, CO_2 can be trapped between packer at depth −1605 m and well screen top level at -1621 m below ground surface. The presence of CO_2 phase in this part results that gas saturation between two sensors be about 0.05 between two pressure drops.

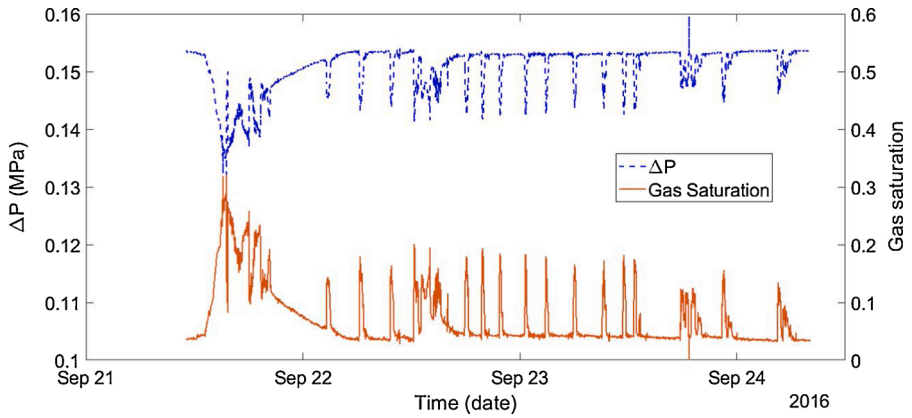

Fig. 6. Pressure difference (blue dashed curve) and interpreted gas saturation (red solid curve) between sensors at 1632.91 m depth and at 1617.35 m depth during the self-release period.

3.2. Results of the numerical modeling

3.2.1. Coupled well-reservoir simulations

3.2.1.1. Scenario 1: Relative permeability as determined from the core samples. In Scenario 1 the relative permeability functions were taken as those measured on Heletz cores (Fig. 5). The resulting simulated pressure at the bottom of the wellbore along with the measured pressure are shown in Fig. 7. The result suggests that the numerical model based on Scenario 1 cannot properly reproduce the process of CO_2 self-release as observed in the experiment. The observed pressure signal exhibits strong pulsation, which is not captured by the simulation. In the simulation, after an initial drop at the start, the pressure increases in three steps. The sudden drop in the beginning is caused by an initial gas accumulation in the wellbore, as shown by the evolution of gas volume percentage at the bottom and the middle of the wellbore (Fig. 8). The following multistep increase in turn is caused by the reduction in wellbore gas saturation (Fig. 8). The gas saturation in the reservoir reduces after the first peak. Both the gas and liquid flow rates decrease quickly after the first peak and eventually reach zero (Fig. 9). At the bottom of the wellbore, the gas stops flowing earlier than the liquid because of self-accelerating effect on CO_2 flow rate is more than the liquid flow rate (Fig. 9).

3.2.1.2. Scenario 2: reduced relative permeability. As it was apparent that Scenario 1 could not reproduce the oscillating pressure behavior, and the geyser-like water−CO_2 outbursts observed in the experiment, the exsolution-reduced gas and liquid relative permeabilities as suggested

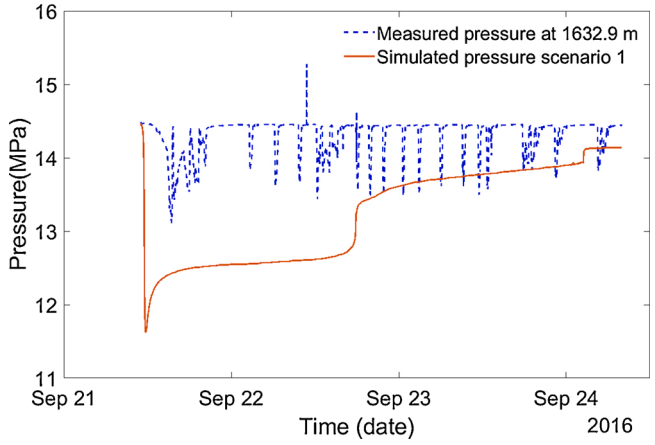

Fig. 7. Measured and simulated pressure (at depth of 1617.35 m) for scenario 1 with relative permeability data obtained from core samples.

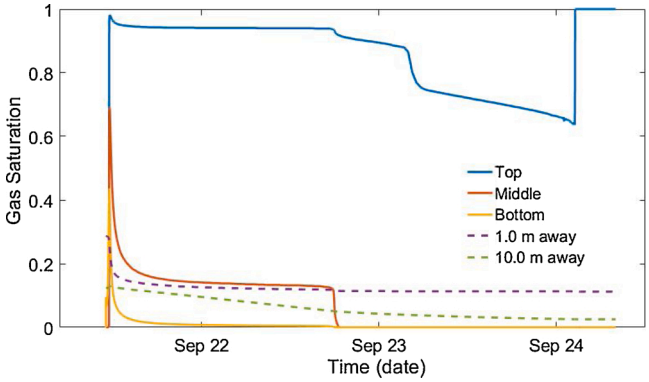

Fig. 8. Simulated gas saturation at three levels in the well (top, middle, and bottom), and two locations in the upper layer of the reservoir for scenario 1 with measured core relative permeability.

by Zuo et al. (2012, 2013) were tested next. In Scenario 2, the CO_2 phase mobility was considered to be negligible and the water mobility in the reservoir was reduced by using the relative permeability functions shown in Fig. 5 (the solid lines). Fig. 10 shows that the numerical model based on the reduced permeability can indeed well reproduce the oscillating pressure behavior observed in the field experiment. It should be pointed out that the model is not intended to capture the early part of the open-well period where only CO_2 is being released, mainly from the wellbore. The result is a significant improvement from that in Scenario 1 and captures well the observed overall behavior. Detailed comparison shows some quantitative differences in the number, duration and size of pressure drops. The size of measured pressure drops is about 0.9 MPa, to be compared to the simulated value of 2.5 MPa, on average. The overestimation of the pressure drop by the model is due to the exclusion of the flow in the uppermost part of the model. As discussed previously, the -194 level of water table was set as constant pressure boundary condition. In reality there is variable flow of CO_2-water mixture in this upper part of the well also as well as in the piping system connecting the well to the outlet tank. If the weight of the 194 m column of CO_2-water mixture and the friction and momentum terms were considered, it would, during a pressure drop, definitely make the pressure at depth much larger than the atmospheric pressure boundary condition that is now used. In order to see the effect of excluding the upper 194 m of wellbore, a simple wellbore model was constructed with T2Well. The upper part was initially assumed to be filled with CO_2 and then one of the events of CO_2 and water leakage event was simulated. The simulations showed that injection of CO_2 and water into to this upper part (rate of CO_2 and water injection was taken from the earlier simulations) creates an overpressure

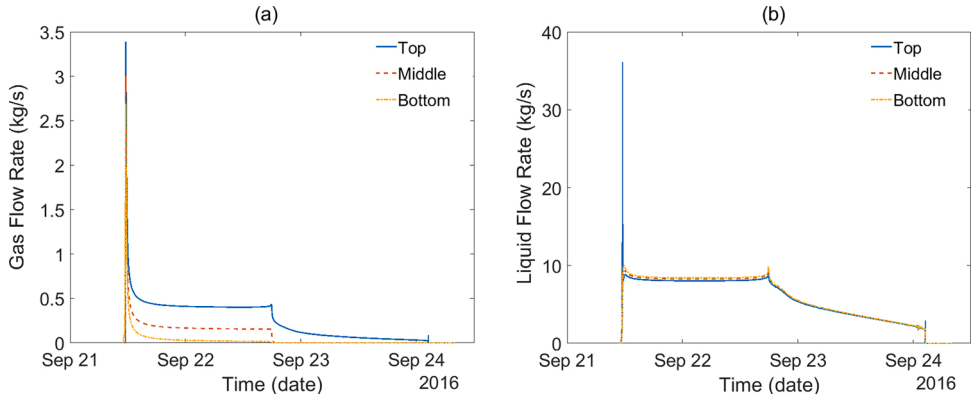

Fig. 9. (a) Simulated gas flow rate and (b) Simulated liquid flow rate at three levels in the well (top, middle, and bottom) for scenario 1 with measured core relative permeability.

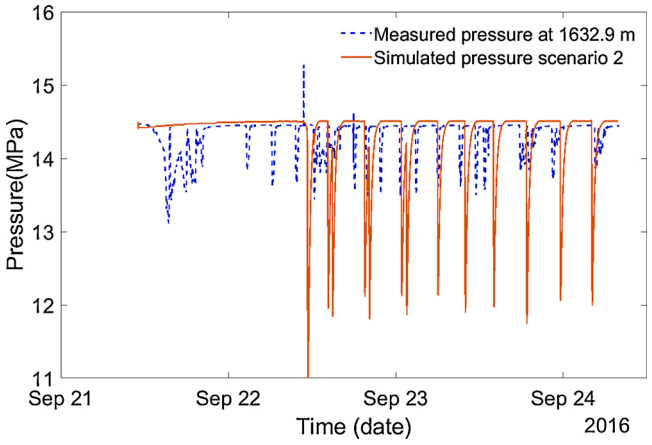

Fig. 10. Measured pressure (blue dash line) and numerically simulated pressure (at depth of 1617.35 m) for Scenario 2 with modified relative permeability.

of about 2.2 MPa at the -194 m below ground level, at the time when the pressure is at the minimum at the bottom of the well. A more simplistic evaluation of assuming the uppermost 194 m of the wellbore to contain 15 % of CO_2 and 85 % water, would in turn result in a pressure of 1.6 MPa at the −194 m level. In the previous modeling we had assumed the pressure at that point to be at atmospheric pressure *i.e.*1 bar. This difference is of the same order of magnitude as the difference between measured and modelled pressure low points in Fig. 14b.

The simulated flow rates of the liquid and gas phases during the self-release period are shown in Fig. 11. It can be seen that the observed intermittent CO_2 production from the wellbore is also captured well. A typical CO_2 release event begins with a sudden eruption at the top of the wellbore followed by a gradual decrease to zero. The CO_2 mass flow rate at the bottom of the wellbore is about 0.06 kg/s at the peak of each jump (Fig. 11a). Both the gas and the liquid flow rates are higher at the top than at the bottom of the wellbore (Fig. 11b, c). The gas flow rate is higher at the top than at the middle and the bottom of the wellbore, which can be attributed to the acceleration caused by the density reduction and the formation of slug flow regime (Fig. 11c). This process is known as the self-acceleration effect (Pan et al., 2011a).

As the relative permeability of gas in the reservoir is zero, the CO_2 gas flow rates at the bottom are zero during the individual production events. The CO_2 flows in vicinity of the wellbore in reservoirs in the form of dissolved CO_2 in brine. As aqueous CO_2 exsolves due to pressure reduction, CO_2 bubbles form. CO_2 bubbles flow upwards because of buoyancy forces that depend on the density difference of brine and CO_2(g).

Fig. 12 shows the simulated volume fractions of CO_2 between the two pressure sensors in the wellbore that can be compared to the corresponding data values in Fig. 6. Also, here a very good general agreement can be observed between the simulated CO_2 volume fractions and the data-estimated volume fractions based on the pressure difference between the two sensors in the well (Fig. 6). The estimated volume fraction at the peaks is between 5% and 10 % (except the first peak associated with the eruption of gas only); the simulated values are about 7%.

3.3. Wellbore flow simulation

The previous results indicate that the overall oscillating behavior could be well captured with the Scenario 2 model. All the critical elements, *i.e.* the oscillating pressure, the level of gas saturation and the oscillating outbursts of water and CO_2 were captured, indicating that the conceptual model and assumptions are correct. The exact lengths of the outburst periods were, however, not captured. For the overall interpretation of the Residual Trapping Experiment I (Niemi et al., 2020; Joodaki et al., 2020a,b) it is of interest to get an as accurate estimate of the CO_2 lost during this self-release period as possible. We therefore carried out an additional analysis attempting to match the pressure oscillations in greater detail, by simulating the processes in the wellbore alone using T2well/ECO2N. For this modeling we use a variable inlet flow rate for CO_2 and water as the boundary condition at the bottom of the wellbore and atmospheric pressure at the top of the well. Similar to the previous coupled reservoir-wellbore model, the top of model is considered at 194 m below ground level in the wellbore flow modeling and is a specified pressure boundary condition. The inlet flow rates for CO_2 and water are assigned similar triangular shapes to the flow rates obtained from the Scenario 2 simulation (Fig. 11). The height and duration of the flow rates were manually adjusted to match duration of each pressure drop (Fig. 13a).

The simulated pressure from the well model along with the experimental data is shown in Fig. 13b, showing an improved agreement in the duration of the events. During the calibration of well model, it is assumed that the size of pressure drops in the model is larger than that in the field data in order to consider the pressure dissipation by gravity and friction in part of the well that was not modeled.

Fig. 14 shows the measured and modelled cumulative volume of water discharged from the well during the self-release period. At the end of the period the field measurement shows a total of 140 m^3 of discharged water, while the corresponding model result is 150 m^3 (Fig. 14a). For comparison, the total volume released with the first Scenario 2 model, without detailed calibration of the peaks, was 100.9 m^3. Based on the detailed calibrated model the estimated total CO_2 discharged from the system is about 10.14 tons at the end of the self-release period. Overall, this is a significant amount of the 100 tons of CO_2 injected in order to create the residually trapped zone.

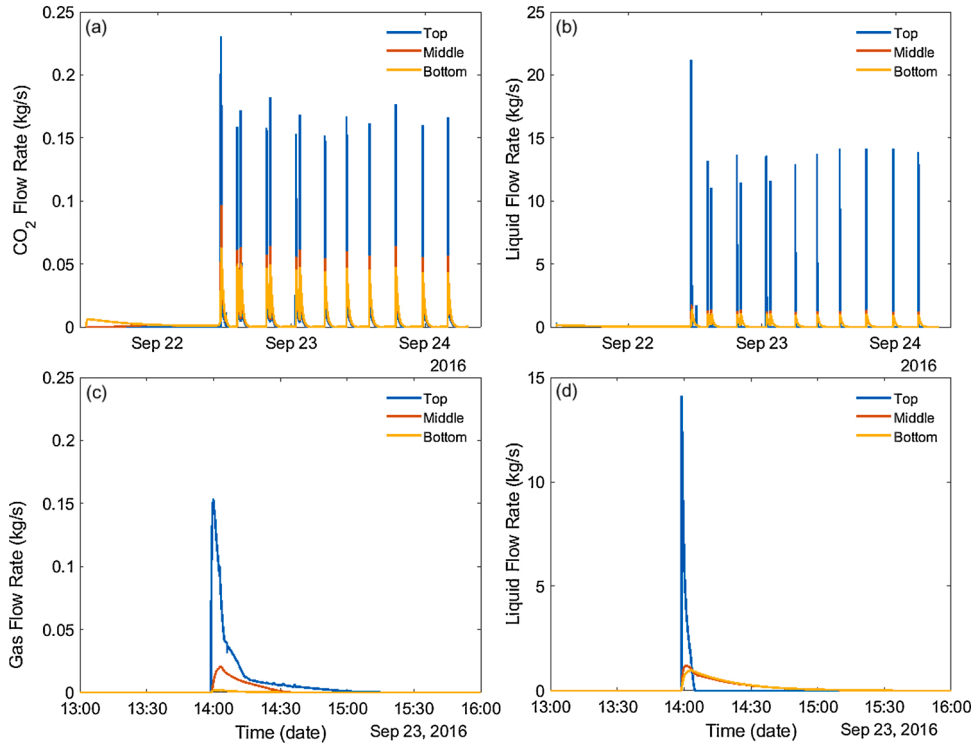

Fig. 11. Simulated fluid production with Scenario 2. (a) Simulated CO_2 flow rate and (b) simulated liquid flow rate at three levels in the well (top, middle, and bottom). (c) Simulated gas flow rate and (d) liquid flow rate during a single event of production of fluids.

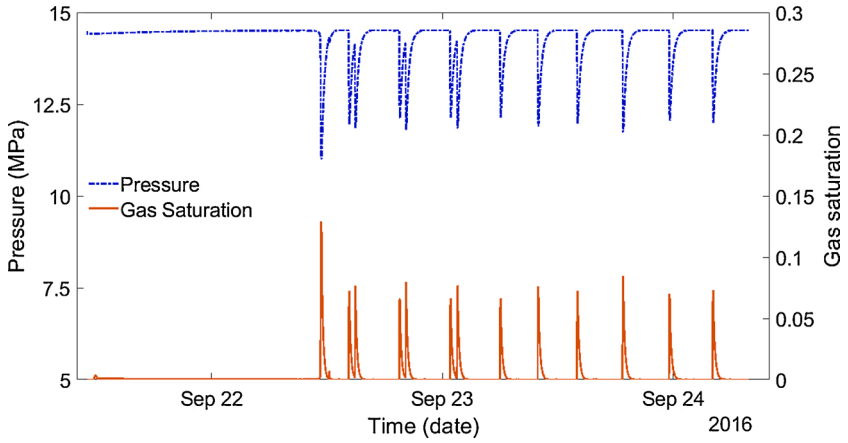

Fig. 12. The simulated volume fraction of CO_2 between the two sensors along with simulated pressure.

4. Discussion

The objective of this study has been to analyze and understand the period of geyser-like self-release of CO_2 and water during the Heletz Residual Trapping Experiment I (Niemi et al., 2020). The generation of the residually trapped zone of CO_2 in the experiment consisted of three main stages: injection of supercritical CO_2 into the formation, opening of the injection well to the atmospheric pressure so that CO_2 and water were self-released into atmosphere in a geyser-like manner and finally, removal of the remaining mobile CO_2 by means of active pumping. Understanding the self-release stage and the associated loss of CO_2 from the system is critical for the analysis of the experiment and requires the coupled analysis of the well-reservoir behavior. For this reason, in the present study, a coupled wellbore-reservoir simulation was carried out by using the T2Well/ECO2N model (Pan et al., 2011b), in order to analyze and understand the self-release period.

In the first model (Scenario 1) the relative permeabilities were presented as measured on Heletz cores by Hingerl et al. (2016). These simulations did, however, not at all capture the oscillating pressure response observed in the measured data (Fig. 7). The simulated pressure drop was much more even and generally also larger than the measured values, implying that the model would overestimate the CO_2 production during the self-release stage.

In order to capture the observed oscillating behavior of pressure and CO_2 outflow, the CO_2 inflow from the reservoir into the well had to be reduced, in comparison to the previous 'first-estimate' model. This inflow is controlled by the mobility of fluids in the area near the wellbore. The mismatch between the simulation results and the field data in Scenario 1 suggests that the relative permeability measured in core samples may not be representative of the two-phase hydraulic properties near the wellbore during the period of well opening. One possible explanation for the mobility reduction is perforation damage resulting

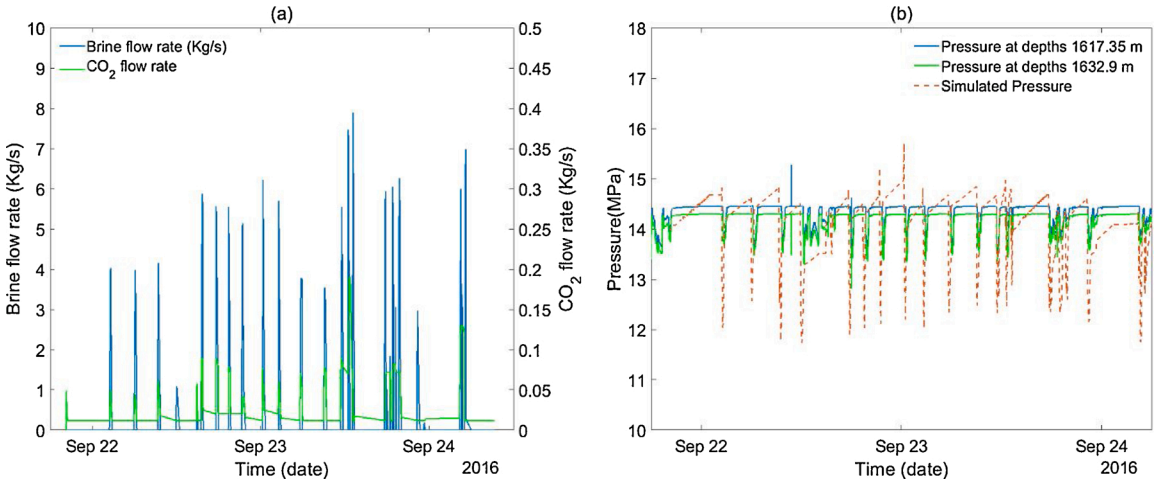

Fig. 13. (a) Adjusted brine and CO_2 flow rates and (b) Measured and simulated pressure. Simulation with the detailed wellbore model.

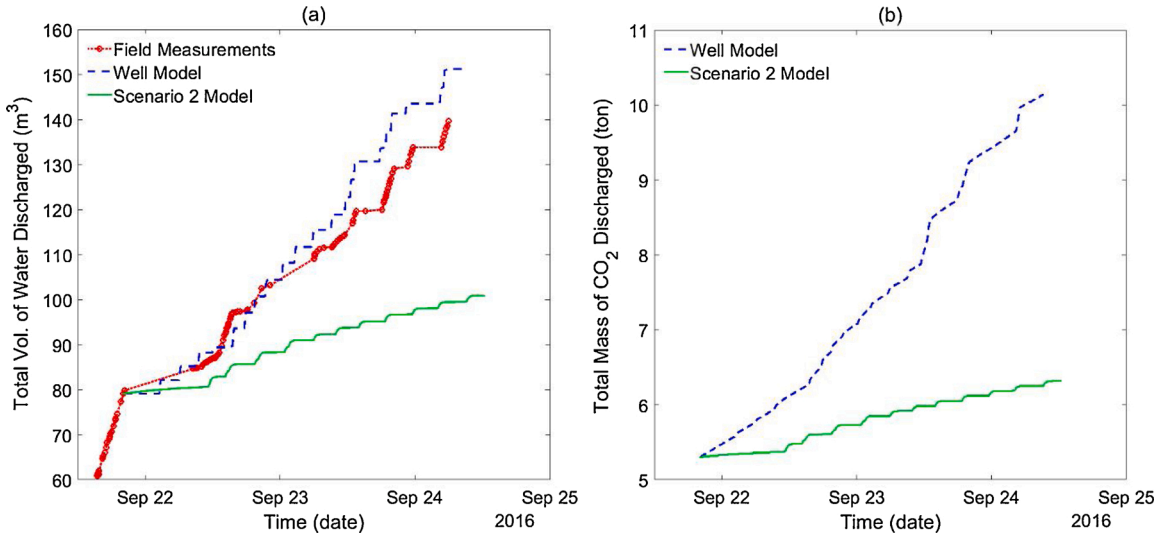

Fig. 14. (a) Measured and calculated cumulative volume of water discharged from the top of the well and (b) calculated total amount of CO_2 discharge.

from grain crushing and fines accumulation (Sharma, 2000). Even clean perforation channels show a thin region of reduced permeability around them which is known as crushed or compacted zone (Klotz et al., 1974; McLeod, 1983). Another possible explanation is formation of micro-bubbles or nucleation of gas phase near the well-reservoir area due to depressurization or temperature variations (El Yousfi et al., 1997; Firoozabadi and Kashchiev, 1996). This could result from the pressure reduction when the well is opened to the atmospheric pressure. The laboratory experiments by Zuo et al. (2012) have indicated that even small amounts of exsolved CO_2 may act as a barrier, preventing further migration of supercritical CO_2 or even blocking possible leakage paths (Zuo et al., 2012).

Therefore, the effect of reduced relative permeabilities (see curves of scenario 2, Fig. 5) due to exsolution as proposed by Zuo et al. (2012) was tested. With this model a significantly improved agreement with the measured data was achieved and the model did well capture the observed oscillating behavior. All the critical elements, *i.e.* the oscillating pressure, the level of gas saturation in the wellbore and the geyser-like outbursts of water and CO_2 could be captured, indicating that the conceptual model and assumptions are correct (Figure 10, 11 and 12).

Even though the Scenario 2 model reproduced all the general behaviors of pulsating CO_2 and water release observed in the field very well, there were some quantitative differences in the exact duration and number of the oscillation events as well as the downhole pressure difference (Fig. 12). An exact agreement would require precise knowledge of the prevailing heterogeneous hydraulic properties, the exsolution-reduced relative permeabilities, and the initial CO_2 saturation in the reservoir at the onset of the events, which is not available. In order to get an as good as possible estimate of the water and CO_2 lost during this self-release period, additional one-dimensional well simulations were done. In these simulations the observed behavior of the coupled well-reservoir model was used as the flow input and the model was calibrated against the field-measured pressure oscillation behavior and the amount of water and CO_2 lost from the system was obtained, providing a better agreement with the measured water outflow (Fig. 14).

The calculated water discharge (Fig. 14a) with this calibrated model showed a very good agreement with the measured water discharge (less than 5% error). The calculated discharge of CO_2 is about 10 tons at the end of self-release flowing out, to be compared to the total of 100 tons of injected CO_2.

5. Conclusions

In this study, we have used the coupled well-reservoir simulator T2Well/ECO2N to understand the geysering behavior of CO_2 and brine

leakage during the self-release stage of the Residual Trapping Experiment I at the Heletz, Israel pilot injection site. The behavior could be explained by CO_2 exsolution from brine when the pressure in the vicinity of the well is lowered due to well opening. We have furthermore shown that low relative permeabilities of CO_2 and brine are needed to simulate the observed phenomena. By using the reduced mobility of fluids as observed in exsolution-related laboratory experiments, all the key behaviors, *i.e.* the pressure oscillation, the oscillating outbursts of water and CO_2 as well as the oscillating gas saturation in the wellbore could be matched. The reduction of mobility in the reservoir can be linked to the formation of gas bubbles in the reservoir area surrounding the wellbore, occurring due to exsolution. This study demonstrates that for a sufficient understanding of the processes near a wellbore during CO_2 leakage through the well, coupled well-reservoir simulators are needed. The observed behavior has significance for any possible leakage events where CO_2 could leak to the atmosphere through a well or even a fracture zone, either intentionally like in the present experiment or unintentionally, for instance through abandoned wells.

CRediT authorship contribution statement

Farzad Basirat: Formal analysis, Methodology, Conceptualization, Visualization. **Zhibing Yang:** Writing - review & editing. **Jacob Bensabat:** Data curation, Resources, Investigation, Project administration. **Stanislav Levchenko:** Data curation, Resources, Investigation. **Lehua Pan:** Software, Methodology, Writing - review & editing. **Auli Niemi:** Writing - review & editing, Data curation, Investigation, Supervision.

Declaration of Competing Interest

The authors declare that they have no known competing financial interests or personal relationships that could have appeared to influence the work reported in this paper.

Acknowledgment

The authors would like acknowledge the financial support from the TRUST project (European Community's Seventh Framework Programme FP7/2007-2013 under grant agreement no 309607) and Swedish Energy Agency grant no 43526-1.

Appendix A. Supplementary data

Supplementary material related to this article can be found, in the online version, at doi:https://doi.org/10.1016/j.ijggc.2020.103162.

References

Ennis-King, J., LaForce, T., Paterson, L., Dance, T., Jenkins, C., Cinar, Y., 2017. Interpretation of above zone and storage zone pressure responses to carbon dioxide injection in the 2016 CO2CRC field test. Energy Procedia 114, 5671–5679. https://doi.org/10.1016/j.egypro.2017.03.1706.

Firoozabadi, Abbas, Kashchiev, Dimo, 1996. Pressure and volume evolution during gas phase formation in solution gas drive process (includes associated papers 38340 and 38565). Spe J. 1 (03), 219–228.

Gouveia, F.J., Friedmann, S.J., 2006. Timing and Prediction of CO2 Eruptions From Crystal Geyser, UT. Lawrence Livermore National Lab.(LLNL), Livermore, CA (United States).

Haese, R.R., LaForce, T., Boreham, C., Ennis-King, J., Freifeld, B.M., Paterson, L., Schacht, U., 2013. Determining residual CO2 saturation through a dissolution test-results from the CO2CRC otway project. Energy Procedia 37, 5379–5386.

Han, Weon S., Lu, M., McPherson, B.J., Keating, E.H., Moore, J., Park, E., Watson, Z.T., Jung, N.-H., 2013. Characteristics of CO2-driven cold-water geyser, C rystal G eyser in U tah: experimental observation and mechanism analyses. Geofluids 13 (3), 283–297.

Hingerl, Ferdinand, F., Yang, Feifei, Pini, Ronny, Xiao, Xianghui, Toney, Michael F., Liu, Yijin, Benson, Sally M., 2016. Characterization of heterogeneity in the Heletz sandstone from core to pore scale and quantification of its impact on multi-phase flow. Int. J. Greenh. Gas. Con. 48 (Part 1), 69–83.

Joodaki, Saba, Yang, Zhibing, Bensabat, Jacob, Niemi, Auli, 2020a. Model analysis of CO_2 residual trapping from single-well push pull test based on hydraulic withdrawal tests – heletz, Residual Trapping Experiment I. Int. J. Greenh. Gas Control. 97 https://doi.org/10.1016/j.ijggc.2020.103058. In this issue.

Joodaki, Saba, Moghadasi, Ramin, Basirat, Farzad, Yang, Zhibing, Bensabat, Jacob, Niemi, Auli, 2020b. Model analysis of CO_2 residual trapping from single-well push pull test – Heletz, Residual Trapping Experiment II. Int. J. Greenh. Gas Control. 101 https://doi.org/10.1016/j.ijggc.2020.103134. In this issue.

Klotz, J.A., Krueger, R.F., Pye, D.S., 1974. Effect of perforation damage on well productivity. J. Pet. Technol. 26 (11), 1303–1314.

Krevor, Samuel, Blunt, Martin J., Benson, Sally M., Pentland, Christopher H., Reynolds, Catriona, Al-Menhali, Ali, Ben, Niu., 2015. Capillary trapping for geologic carbon dioxide storage – from pore scale physics to field scale implications. Int. J. Greenh. Gas Control. 40, 221–237.

LaForce, T., Ennis-King, J., Boreham, C., Paterson, L., 2014. Residual CO_2 saturation estimate using noble gas tracers in a single-well field test: the CO_2CRC Otway project. Int. J. Greenh. Gas Control. 26, 9–21.

Lu, Xinli, Watson, Arnold, Gorin, Alexander V., Deans, Joe, 2005. Measurements in a low temperature CO_2-driven geysering well, viewed in relation to natural geysers. Geothermics 34 (4), 389–410.

Lu, Xinli, Watson, Arnold, Gorin, Alexander V., Deans, Joe, 2006. Experimental investigation and numerical modelling of transient two-phase flow in a geysering geothermal well. Geothermics 35 (4), 409–427.

McLeod Jr., Harry O., 1983. The effect of perforating conditions on well performance. J. Pet. Technol. 35 (01), 31–39.

Michels, P.J., Johnson, N.P., Hornung, C.A., Updike, J., 1993. Relationship of management of substance abusers to psychological and practice pattern characteristics of family physicians. Psychol. Addict. Behav. 7 (1), 21–28.

Niemi, Auli, Bensabat, Jacob, Fagerlund, Fritjof, Sauter, Martin, Ghergut, Julia, Licha, Tobias, Fierz, Thomas, Wiegand, Gabriele, Rasmusson, Maria, Rasmusson, Kristina, Shtivelman, Vladimir, Gendler, Michael, 2012. Small-scale CO_2 injection into a deep geological formation at Heletz. Israel." Energy Procedia 23, 504–511.

Niemi, Auli, Bensabat, Jacob, Joodaki, Saba, Hedayati, Maryeh, Yang, Zhibing, Basirat, Farzad, Perez, Lily, Levchenko, Stanislav, Shklarnik, Alon, Ronen, Rona, Goren, Yoni, Tsarfis, Igal, Fagerlund, Fritjof, Rasmusson, Kristina, Hassan, Jawad, Sauter, Martin, Ghergut, Iulia, Gouze, Philippe, Freifeld, Barry, 2020. Characterizing CO_2 capillary trapping in the field by means of single-well push-pull experiments at Heletz, Israel pilot injection site – experimental procedures and data from residual trapping experiments I and II. Paper submitted for review to special edition' Heletz residual trapping experiments. Int. J. Greenh. Gas Control. 101 https://doi.org/10.1016/j.ijggc.2020.103129.

Niemi, Auli, Bensabat, Jacob, Shtivelman, Vladimir, Edlmann, Katriona, Gouze, Philippe, Luquot, Linda, Hingerl, Ferdinand, Benson, Sally M., Pezard, Philippe A., Rasmusson, Kristina, Liang, Tian, Fagerlund, Fritjof, Gendler, Michael, Goldberg, Igor, Tatomir, Alexandru, Lange, Torsten, Sauter, Martin, Freifeld, Barry, 2016. Heletz experimental site overview, characterization and data analysis for CO_2 injection and geological storage. Int. J. Greenh. Gas Control. 48 (Part 1), 3–23.

Niemi, Auli, Bear, Jacob, Bensabat, Jacob, 2017. Geological Storage of CO_2 in Deep Saline Formations, 29. Springer, Berlin.

Pan, L., Oldenburg, C.M., 2014. T2Well-An integrated wellbore-reservoir simulator. Comput. Geosci. 65, 46–55.

Pan, Lehua, Oldenburg, Curtis M., Pruess, Karsten, Yu-Shu, Wu., 2011a. Transient CO_2 leakage and injection in wellbore-reservoir systems for geologic carbon sequestration. Greenh. Gases Sci. Technol. 1 (4), 335–350.

Pan, Lehua, Oldenburg, Curtis M., Wu, Yu-Shu, Pruess, Karsten, 2011b. T2Well/ECO$_2$N Version 1.0: Multiphase and Non-isothermal Model for Coupled Wellbore-reservoir Flow of Carbon Dioxide and Variable Salinity Water. ed. LBNL-4291E.

Pan, Lehua, Webb, Stephen W., Oldenburg, Curtis M., 2011c. Analytical solution for two-phase flow in a wellbore using the drift-flux model. Adv. Water Resour. 34 (12), 1656–1665.

Pan, Lehua, Doughty, Christine, Freifeld, Barry, 2018. How to sustain a CO_2-thermosiphon in a partially saturated geothermal reservoir: lessons learned from field experiment and numerical modeling. Geothermics 71, 274–293.

Paterson, Lincoln, Boreham, Chris, Bunch, Mark, Dance, Tess, Ennis-King, Jonathan, Freifeld, Barry, Haese, Ralf, Jenkins, Charles, LaForce, Tara, Raab, Matthias, Singh, Rajindar, Stalker, Linda, Zhang, Yingqi, 2013. Overview of the CO_2CRC otway residual saturation and dissolution test. Energy Procedia 37, 6140–6148.

Pruess, Karsten., 2008. On CO_2 fluid flow and heat transfer behavior in the subsurface, following leakage from a geologic storage reservoir. Environ. Geol. 54 (8), 1677–1686.

Rasmusson, K., Rasmusson, M., Fagerlund, F., Bensabat, J., Tsang, Y., Niemi, A., 2014. Analysis of alternative push–pull-test-designs for determining in situ residual trapping of carbon dioxide. Int. J. Greenh. Gas Control. 27, 155–168.

Ross, K., 1997. Cold water geysers in southern Utah. The GOSA Sput 11, 14–15.

Sharma, Mukul M., 2000. The nature of the compacted zone around perforation tunnels. In: In SPE International Symposium on Formation Damage Control. Lafayette. Louisiana: Society of Petroleum Engineers.

Shi, Hua, Holmes, Jonathan A., Durlofsky, Louis J., Aziz, Khalid, Diaz, Luis, Alkaya, Banu, Oddie, Gary, 2005. Drift-flux modeling of two-phase flow in Wellbores. Spe J. 10 (01), 24–33.

Watson, Z.T., Han, Weon Shik, Keating, Elizabeth H., Jung, Na-Hyun, Meng, Lu., 2014. Eruption dynamics of CO_2-driven cold-water geysers: crystal, Tenmile geysers in Utah and Chimayó geyser in New Mexico. Earth Planet. Sci. Lett. 408, 272–284.

El Yousfi, A., Zarcone, C., Bories, S., Lenormand, R., 1997. Physical mechanisms for bubble growth during solution gas Drive. In: SPE Annual Technical Conference and Exhibition. San Antonio, Texas: Society of Petroleum Engineers.

Zhang, Yingqi, Freifeld, Barry, Finsterle, Stefan, Leahy, Martin, Ennis-King, Jonathan, Paterson, Lincoln, Dance, Tess, 2011. Single-well experimental design for studying residual trapping of supercritical carbon dioxide. Int. J. Greenh. Gas Control. 5 (1), 88–98.

Zuo, Lin, Krevor, Samuel, Falta, Ronald W., Benson, Sally M., 2012. An experimental study of CO_2 exsolution and relative permeability measurements during CO_2 saturated water depressurization. Transp. Porous Media 91 (2), 459–478.

Zuo, Lin, Zhang, Changyong, Falta, Ronald W., Benson, Sally M., 2013. Micromodel investigations of CO_2 exsolution from carbonated water in sedimentary rocks. Adv. Water Resour. 53, 188–197.